References

1. Raether H *Surface Plasmons on Smooth and Rough Surfaces and on Gratings* (Berlin: Springer-Verlag, 1988)
2. Moskovits M et al., in *Optical Properties of Nanostructured Random Media* (Topics in Applied Physics, Vol. 82, Ed. V M Shalaev) (Berlin: Springer-Verlag, 2002) p. 215
3. Wang Z et al. *Proc. Natl. Acad. Sci. USA* **100** 8638 (2003)
4. Lakowicz J R et al. *J. Phys. D: Appl. Phys.* **36** R240 (2003)
5. Guzatov D V, Klimov V V *Chem. Phys. Lett.* **412** 341 (2005)
6. Bergman D J, Stockman M I *Phys. Rev. Lett.* **90** 027402 (2003)
7. Zia R et al. *Mater. Today* **9** (7–8) 20 (2006)
8. Klimov V V, Guzatov D V *"Opticheskie svoistva trekhosnogo nanoellipsoida i ikh vliyanie na izluchenie atomov i molekul"* ("Plasmon oscillations in ellipsoidal nanoparticles: beyond dipole approximation") (in preparation)
9. Sun Y, Xia Y *Science* **298** 2176 (2002)
10. Klimov V V, Guzatov D V *Phys. Rev. B* **75** 024303 (2007)
11. Klimov V V, Guzatov D V *Kvantovaya Elektron.* **37** 209 (2007) [*Quantum Electron.* **37** 209 (2007)]
12. Klimov V V, Guzatov D V *Appl. Phys. A* **89** 305 (2007)
13. Claro F *Phys. Rev. B* **25** 7875 (1982)
14. Ruppin R *Phys. Rev. B* **26** 3440 (1982)
15. Nordlander P et al. *Nano Lett.* **4** 899 (2004)
16. Ekinci K L, Roukes M L *Rev. Sci. Instrum.* **76** 061101 (2005)
17. Klimov V V, Lambrecht A, arXiv:0712.4067
18. Palik E D (Ed.) *Handbook of Optical Constants of Solids* (Orlando: Academic Press, 1985)
19. Engelbrecht F, Helbig R *Phys. Rev. B* **48** 15698 (1993)
20. Soukoulis C M, Linden S, Wegener M *Science* **315** 47 (2007)
21. Klimov V V *Opt. Commun.* **211** 183 (2002)

PACS numbers: 52.27.Ep, 97.10.Ld, 97.60.Jd
DOI: 10.1070/PU2008v051n08ABEH006596

Electron – positron plasma generation in the magnetospheres of neutron stars

Ya N Istomin

1. Introduction

In this report we discuss the processes of the generation of relativistic electron – positron plasma in magnetospheres of rotating magnetized neutron stars. Both not very strong magnetic fields, $B \simeq 10^{12}$ G, typical for radio pulsars, and superstrong magnetic fields, $B \simeq 10^{14} - 10^{15}$ G, typical for so-called magnetars, are considered. It is shown that superstrong magnetic fields do not suppress particle production. Intervals of neutron star parameters, first of all rotation periods and magnetic field strengths, allowing effective plasma generation have been found.

Neutron stars are the smallest observed stars in the Galaxy. Their radius R is around 10 km (for comparison, the solar radius amounts to 7×10^5 km). So, the ratio of the radius of a neutron star to that of ordinary stars is about 10^{-5}. However, with such a small radius, neutron stars have a mass M on the order of the solar one $M_\odot$, with the average magnitude being $1.4 M_\odot$. The mean density of the neutron star matter is $\bar{\rho} = 3M/4\pi R^3 = 7 \times 10^{14}$ g cm^{-3}, which exceeds the standard nuclear density $\rho_0 = 2.8 \times 10^{14}$ g cm^{-3} by several times ($\bar{\rho} \simeq 2.5\rho_0$). Therefore, a neutron star can be considered as a huge atomic nucleus with a radius of about 10 km. The matter density at the center of the star can exceed the nuclear one by 10 – 20 times. At such densities in the neutron star center, pion, hyperon, and kaon condensations are made possible. The possibility of the appearance of quarks, mostly strange, is also discussed. Such stars are termed strange stars.

The body of a neutron star consists of outer and inner crusts, where the neutronization of matter occurs, and of outer and inner cores. The number of protons and electrons in the inner crust and outer core is much smaller than the number of neutrons, the ratio being of the order of several percent. Neutrons and protons probably form superfluid and superconducting pairs, so that neutron star matter possesses superfluid and superconductive properties. It should also be noted that the gravitational energy of a neutron star amounts to a substantial fraction of its rest energy: $E_g = GM^2/R \simeq 5 \times 10^{53}$ erg $= 0.2Mc^2$, where G is the Newtonian constant of gravitation.

The existence of neutron stars was predicted by Baade and Zwicky [1] in 1934, two years after the discovery of neutrons. Despite their small size, neutron stars are among the most active stars, radiating energy in the entire electromagnetic spectral range from radio waves to ultra-high energy photons beyond 1 TeV.

Neutron stars were discovered in 1967 by Bell and Hewish [2] as sources of periodic radio emission — radio pulsars. In 1974, Hewish was awarded the Nobel Prize in Physics for his decisive role in the discovery of pulsars.

Presently, more than 1500 radio pulsars are known. Their pulse-repetition intervals, i.e., the periodicity of recurring radio pulses, are very stable and span the range from 1.5 ms to 8.5 s. The high stability and small intervals can only be explained by the rotation of a small body with radius $R < 5 \times 10^7$ cm. Only neutron stars have such small radii. A constant increase in the pulse-repetition intervals P of radio pulsars with time is also observed, $\mathrm{d}P/\mathrm{d}t \simeq 10^{-15}$ s s^{-1}, implying a loss in the rotational energy of a neutron star. The measured energy loss $\mathrm{d}E/\mathrm{d}t = (2\pi)^2 I P^{-3}\,\mathrm{d}P/\mathrm{d}t$ for the standard moment of inertia $I = 10^{45}$ g cm^2 of a neutron star is on the order of $\mathrm{d}E/\mathrm{d}t \simeq 4 \times 10^{31}$ erg s^{-1}. However, rapidly rotating neutron stars actually lose much higher energy. For example, the Crab Nebula pulsar emits 10^{38} erg s^{-1}, which is by many orders higher than the solar luminosity. The energy emitted in the radio frequency band amounts to only a tiny fraction, $10^{-5} - 10^{-6}$, of the total energy losses. The most powerful radio pulsars also radiate in other spectral ranges, including the optical, X-ray, and gamma-ray ranges. The emission power increases with frequency, but nevertheless remains much smaller than the total energy losses. The question arises as to what is mainly emitted by a rotating neutron star?

In addition to being radio pulsars, neutron stars are also the sources of

(a) powerful X-ray emission, both periodic (X-ray pulsars) and irregular. These are neutron stars in close binary stellar systems in which the star-companion provides the neutron star with matter accreting onto it. The energy liberated during accretion amounts to $\simeq 0.2$ of the rest energy of the infalling flux of matter;

(b) gamma- and X-ray bursts. These are anomalous X-ray pulsars (AXPs) and soft gamma repeaters (SGRs). Both these groups are combined into one class of the so-called magnetars. They comprise neutron stars with ultrahigh surface magnetic fields of $10^{14} - 10^{15}$ G;

(c) steady X-ray emission from central compact objects (CCOs) in supernova remnants. These are neutron stars formed during the core collapse of pre-supernova stars;

(d) very faint optical emission. These are nearest radio-quiet isolated neutron stars;

(e) sporadic radio bursts from rotating radio transients (RRATs). These are neutron stars which are not steady working radio pulsars;

(f) unusual gamma- and X-ray emission from sources like Geminga (Gemini gamma-ray source).

The study of neutron stars solves and provides the possibility to solve a number of fundamental physical problems. These include first of all the analysis of the equation of state of superdense matter with $\rho > \rho_0$. The equation of state (up to now, more than ten different equations of state have been proposed theoretically) determines the form of the dependence $M(R)$ of the mass M of a neutron star on its radius R. Masses of neutron stars are measured with a good accuracy in binary systems, their radii being inferred from intensity measurements of the emission from the neutron star surface. Up to the present, however, the accuracy of measurements of radii and masses of neutron stars has been insufficient for the unique determination of the equation of state of the superdense matter.

The superfluidity of neutron matter can be examined by measuring interruptions in the rotation period of a radio pulsar during neutron star rotation braking (glitch). In some cases, the interruption dynamics is explained well by the unpinning of a superfluid vortex from the stellar core. The evolution of the magnetic field 'frozen' in the star allows conclusions about the superconductivity in the neutron star core.

In strong magnetic fields B pertinent to neutron stars, $B > 10^{12}$ G, the structure of matter is unusual. In such fields, the cyclotron radius of atomic electrons is smaller than the Bohr radius, and the atoms are strongly compressed in the direction perpendicular to the magnetic field and take the form of a needle. The properties of matter formed by such atoms can be judged from the interaction of the neutron star surface, where the matter density reaches 10^5 g cm^{-3}, with its magnetosphere.

Very importantly, observations of neutron stars as radio pulsars allow the checking of General Relativity through measurements of post-Newtonian corrections to the dynamics of motion of two neutron stars in a close binary system. For example, a measured decrease in the orbital period of the pulsar PSR B 1913+16 amounted to $\mathrm{d}P_{\mathrm{orb}}/\mathrm{d}t = -2.4086\times10^{-12}$ s s^{-1}, which corresponds to a decrease in the binding energy of the stars due to their emission of gravitational waves. In 1993, R A Hulse and J H Taylor, Jr. were awarded the Nobel Prize in Physics for the discovery of a new type of pulsar, a discovery that has opened up new possibilities for the study of gravitation. The timing, i.e., the precise measurement of the time of arrival of individual pulses, is now so accurate that several of the most stable radio pulsars can be used to construct a frequency standard more stable than current atomic clocks. Measurements of the retardation of a radio signal at different frequencies and its polarization are used to determine the parameters of interstellar medium: the electron number density, the magnetic field strength, and inhomogeneities. By this is meant that it is also possible to probe the nearby environments of radio pulsars. The timing of radio pulsars allows studies of the cosmic background of gravitational waves.

Finally, observations of active neutron stars enable us to investigate electrodynamic processes in superstrong magnetic fields $B > 10^{12}$ G typical for neutron stars. Here, we will consider the processes of plasma generation in magnetospheres of rotating magnetized neutron stars.

2. The magnetic field of neutron stars

Observations revealed that the energy lost by a rotating neutron star as radio pulsar is mainly spent on the formation of the flux of relativistic particles called the pulsar wind. Thus, it is precisely these relativistic particles that feed the entire Crab Nebula. The flux of such particles is about 10^{40} particles per second. Observations of the unique binary system consisting of two radio pulsars J0737-30039 A, B allow one to show how the pulsar wind from the more powerful pulsar compresses the magnetosphere of the star-companion several dozen-fold. The heating of the star-companion to the millisecond pulsar 1957+20 at orbital phases where the companion side turned toward the pulsar has also been observed.

However, for a long time the activity of a rotating neutron star was thought to be connected not with the wind emission but with the emission of the so-called magneto-dipole wave, an electromagnetic wave generated by the rotating magnetic dipole frozen in the star. The emission power of the magneto-dipole radiation, $\mathrm{d}E/\mathrm{d}t = 2\Omega^4\mu^2\sin^2\chi/3c^3$, was matched with the rotational energy losses of the neutron star. Here, $\Omega = 2\pi/P$ is the rotation frequency of the star, μ is its magnetic moment, and χ is the angle between the rotation axis and the magnetic dipole axis. The derived estimate of the surface magnetic field intensity $B = (P\,\mathrm{d}P/\mathrm{d}t_{-15})^{1/2}\times10^{12}$ G exactly matched the expected values. (The notation $\mathrm{d}P/\mathrm{d}t_{-15}$ means the rotational braking in units of 10^{-15} s s^{-1}).

The idea that the activity of rotating neutron stars is related to the presence of a strong magnetic field $B \simeq 10^{12}$ G was put forward by V L Ginzburg almost immediately after the discovery of radio pulsars. Indeed, assuming magnetic flux freezing, during the fast compression of the pre-supernova star by 10^5 times the magnetic field intensity increases by 10^{10} times. So, from the 100-G magnetic fields of ordinary stars we arrive at the above estimate of neutron star magnetic fields. Moreover, during the cooling of a neutron star after a supernova explosion, the magnetic field can be generated in the stellar core by the current of electrons carrying the heat flux. Observations of absorption cyclotron lines in the spectra of some X-ray sources also indicate a magnetic field strength of order 10^{12} G on the neutron star surface. The upper limit of the magnetic field intensity of a neutron star, 10^{18} G, is given by equating the magnetic field energy to the gravitational energy E_{g} of the neutron star.

As mentioned above, there are neutron stars belonging to a rather small but very active class, which demonstrate bright bursts of gamma- and X-ray emission and have significantly stronger magnetic fields than ordinary pulsars. Such stars rotate comparatively slowly with the periods $P \simeq 5-10$ s but undergo braking much faster, $\mathrm{d}P/\mathrm{d}t \simeq 10^{-10}-10^{-12}$ s s^{-1}. Their energy is caused by magnetic fields, not by rotation. The X-ray flux from such a star, $W_{\mathrm{x}} \simeq 10^{35}-10^{36}$ erg s^{-1}, is much higher than the rotational energy losses defined as $I\Omega\,\mathrm{d}\Omega/\mathrm{d}t$. The energy stored in the magnetic field, $\int(B^2/8\pi)\,\mathrm{d}V$, is also larger than the rotational energy $I\Omega^2/2$ of the star. This suggests that the activity of such neutron stars is due to their magnetic fields and not the rotational energy, as is the case for ordinary radio pulsars. Such stars are thus termed magnetars.

The strong magnetic field in the neutron star magnetosphere provides conditions for plasma generation and the formation of a wind — the flux of relativistic electrons and positrons emitted by active stars.

3. Plasma generation

Effective particle creation begins at magnetic field intensities close to the intensity of a so-called critical magnetic field:

$$B_c = \frac{m^2 c^3}{e\hbar} = 4.4 \times 10^{13}\ \mathrm{G}\,.$$

Here, m and e are the mass and charge of an electron, c is the speed of light, and $\hbar$ is the Planck constant. In such a magnetic field, the distance between the adjacent Landau levels is equal to the electron rest energy: $\hbar\omega_c = mc^2$. In such an electric field, the vacuum becomes unstable and electron – positron pair creation begins. The probability of one-photon pair creation in the magnetic field is given by

$$w = bB\sin\beta\exp\left(-\frac{8}{3Bk\sin\beta}\right), \quad B < 1,$$

where β is the angle between the photon wave vector and the direction of the magnetic field, k is the photon wave vector in units of the inverse electron Compton wavelength, the magnetic field intensity is measured in units of the critical magnetic field intensity, and b is a constant. Pair creation occurs above the threshold value of $k\sin\beta > 2$. It is seen that even in not very strong fields, $B < 10^{-2}$, typical in radio pulsars, photons with energy $k > 10^2$ effectively create pairs. In a strong magnetic field $B > 1$, pair creation probability is even higher:

$$w = bB\exp\left(-\frac{k^2\sin^2\beta}{2B}\right), \quad B > 1,$$

and electron – positron pairs form immediately after reaching the threshold.

Relativistic particles in the star magnetosphere rapidly lose transversal momentum due to synchrotron emission and move along the magnetic field. The magnetic field lines have a large curvature; the radius of curvature ρ near the surface changes from the stellar radius ($\simeq 10^6$ cm) at the equator up to about 10^8 cm near the pole. Particles moving along a curved trajectory emit so-called curvature photons with energies $k = 3\gamma^3/2\rho \simeq 10^4$, which is sufficient for subsequent pair creation. Here, γ is the Lorentz factor of a particle, and the radius of curvature is measured in units of the electron Compton wavelength $\hbar/mc$. Charged particles acquire significant energy (with Lorentz factors up to $\gamma \simeq 10^7$) by moving in the electric field E that appears in the rotating magnetosphere, $E \simeq \Omega RB/c$. The curvature photons, which initially propagate along the magnetic field lines, after passing the length l acquire the threshold angle β: $l/\rho = 2/k$, due to the field line curvature. In a strong magnetic field $B > 1$, the length l is the photon mean free path for pair creation. In a weak magnetic field $B < 1$, the mean free path is somewhat longer, $l = 8\rho/3kB\Lambda$, where Λ is a logarithmic factor ranging $\Lambda \simeq 10-15$. In this way, the electron – positron cascade in the neutron star magnetosphere is formed, as shown in Fig. 1.

In a weak magnetic field $B < 1$, the cascade strengthens due to particles being created at high Landau levels and emitting so-called synchrophotons during the transition to the ground level. These additional photons significantly increase the photon number. In a strong magnetic field $B > 1$, particle creation occurs either on the ground or on the first level, depending on the photon polarization.

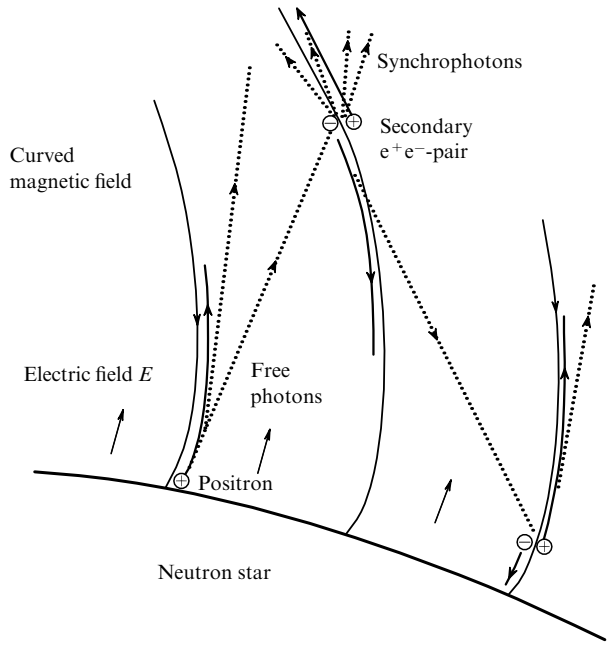

Figure 1. Schematic of the process of creation of an electron – positron pair in the magnetosphere of a neutron star near its surface. Particles are accelerated by the electric field, move along the magnetic field lines, and radiate curvature photons which, by crossing the magnetic field lines, produce electron – positron pairs. In a weak magnetic field $B < B_c$, particles created change to the ground Landau level and emit synchrophotons. In a strong magnetic field, particles are created on the ground or on the first Landau level.

Generally, radiation processes in a strong magnetic field greatly depend on photon polarization. Two polarizations are possible: (1) the longitudinal one, where the electric field of a photon lies in the plane $(\mathbf{k}, \mathbf{B})$ and has a nonzero projection onto the magnetic field, and (2) the transversal one, where the electric field is orthogonal to both the $\mathbf{k}$ and $\mathbf{B}$ vectors.

In a field $B > 1$, the decay of a transverse photon into two longitudinal ones, $k_\perp \to k_{1\parallel} + (k - k_1)_\parallel$, is possible. It had been thought earlier that these two facts, viz. the absence of synchrophotons and the radiation decay of a photon, suppress the plasma generation in a strong magnetic field of magnetar magnetosphere. This seemed to have been confirmed by observations — no magnetars were known to radiate radio emission. However, very low-frequency observations carried out at $\simeq 100$ MHz at the Pushchino Radio Astronomical Observatory of LPI have shown that there is an unusual radio emission from two magnetars [3, 4]. In addition, the anomalous X-ray pulsar (magnetar) XTE 1810-197 started to act as a powerful pulsar after the X-ray burst in 2003 [5]. In 2007, a magnetar emitting in the radio band was also discovered. This means that the generation of *dense* plasma in magnetar magnetospheres with a strong magnetic field $B > 1$ is also possible, as in pulsar magnetospheres with $B < 1$.

A plasma is called dense if the number density of particles exceeds some value called the Goldreich – Julian density n_{GJ} [6], which separates the vacuum magnetosphere of a neutron

star, where a nonstationary electromagnetic field is generated (magneto-dipole wave), and the stationary magnetosphere filled with plasma:

$$n_{\mathrm{GJ}} = -\frac{\mathbf{B\Omega}}{2\pi ce}.$$

This density near the neutron star surface, both in pulsars and magnetars, is of the order of 10^{12} cm^{-3}. Cascade creation of electrons and positrons in the magnetosphere of a radio pulsar leads to a number density much higher than n_{GJ}. The plasma particle multiplicity $\lambda = n/n_{\mathrm{GJ}}$ reaches values of $\lambda = 10^4 - 10^5$ [7].

In magnetars with a strong magnetic field $B > 1$, the plasma particle multiplicity also turned out to be comparable with that in radio pulsars [8]. Although for $B > 1$ there is no second generation of particles, i.e., those created by synchrophotons, the number density of the first-generation particles created by the curvature photons is proportional to the magnetic field strength, $n \propto B$, which compensates for the lack of synchrophotons in a high magnetic field. The photon radiation decay leads to the 100% polarization of gamma quanta which become longitudinally polarized [8].

Thus, a strong magnetic field does not suppress plasma generation, as was thought before. The only factor suppressing plasma particle creation in magnetars is their slow rotation. On average, the rotation periods of magnetars is larger by two orders of magnitude than those of radio pulsars. Thus, the size of the polar cap where plasma is generated, $\simeq R(\Omega R/c)^{1/2}$, decreases by one order of magnitude. This increases the radius of curvature ρ of the magnetic field lines (at the dipole axis ρ is infinite). As a result, the energy range of electrons and positrons created becomes smaller. The minimum Lorentz factor $\gamma_{\min} = \rho/R$ increases, while the maximum one $\gamma_{\max} = 3\gamma_0^3/4\rho$ decreases. The energy $\gamma_0 mc^2$ equals the energy that particles acquire from a longitudinal electric field induced in the polar cap region. At $\gamma_{\max} \simeq \gamma_{\min}$, plasma generation in magnetars almost stops. This condition determines the range of parameters, the neutron star rotation period P and the magnetic field intensity B, where dense plasma generation is possible in magnetar magnetospheres:

$$P\left(\frac{B}{10^{12}\,\mathrm{G}}\right)^{-3/7} < 1 \text{ s}.$$

For radio pulsars, a similar boundary was determined in paper [7] (see also the book [9]): $P(B/10^{12}\,\mathrm{G})^{-8/15} < 1$ s. The $(P, \mathrm{d}P/\mathrm{d}t)$ diagram for radio pulsars and magnetars, in which plasma generation boundaries are shown, is presented in Fig. 2. The magnetic field intensity and the rotation braking is related by the formula $B = (P\,\mathrm{d}P/\mathrm{d}t_{-15})^{1/2} \times 10^{12}$ G.

4. Conclusion

Observations of radio pulsars provide the possibility to explain how plasma generation occurs in magnetospheres of neutron stars. This possibility emerged during observations of a small group of so-called switch-off pulsars. These are pulsars in which radio emission temporarily disappears and then appears again. Such 'radio-quiet' and 'radio-loud' phases occurs at all times of observations. For example, careful observations of the pulsar PSR B1931+24, which is quiet for 20–25 days and then switches on for 5–10 days, showed that its rotation braking is significantly different during the quiet and loud phases [10]. The braking during

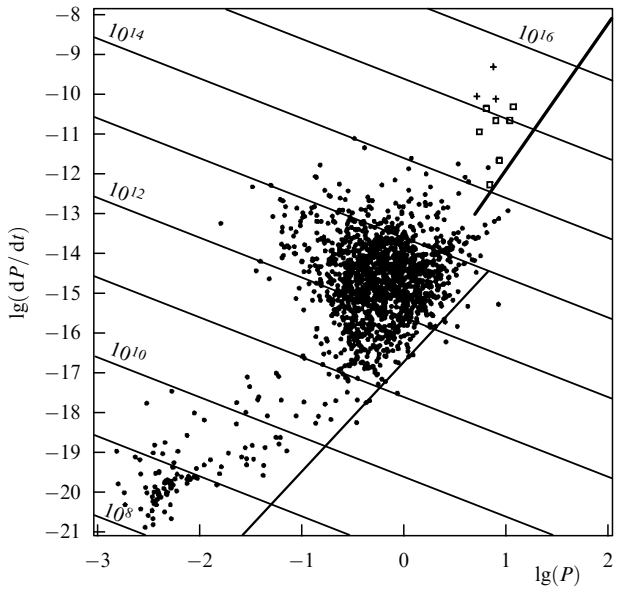

Figure 2. The $P - \mathrm{d}P/\mathrm{d}t$ diagram with boundary lines for effective pair creation. Circles are radio pulsars, while crosses and squares are magnetars. The thin line marks the plasma generation boundary for radio pulsars, $\mathrm{d}P/\mathrm{d}t \propto P^{11/4}$ [7], and the thick line is the plasma generation boundary for magnetars, $\mathrm{d}P/\mathrm{d}t \propto P^{11/3}$ [8].

the radio-loud phase is 1.5 times as effective as during the radio-quiet one. The explanation for this is that the radio emission is related to plasma generation, and the rotational energy of the neutron star is spent on the generation of the pulsar wind. The absence of radio emission, in turn, implies that no plasma is generated and the rotational energy is spent on the generation of magneto-dipole waves [11]. Hence, the energy losses are very different. Should one catch the moment of the switch-on, one could observe the development of cascade plasma generation, which should show up in the intensity and spectral range of the radio emission. At the switch-off moment, which lasts less than 10 s, one could observe the interaction of the magneto-dipole radiation with the pulsar wind. The point is that electromagnetic radiation propagates with the speed of light, faster than the wind, and when catching up with the wind the radiation starts interacting with it. The magnetic field of the radiation excites synchrotron radiation of relativistic particles in the wind. Measurements of the intensity and spectral range of such a radiation would allow the determination of the particle number density and particle energy spectrum in the wind.

In conclusion, we should note that the observations of neutron stars and the theory of the observed phenomena provide us with a fundamental understanding of the behavior of matter under extreme conditions, in particular, in superstrong magnetic fields.

References

1. Baade W, Zwicky F *Proc. Natl. Acad. Sci. USA* **20** 259 (1934)
2. Bell S J, Hewish A *Nature* **213** 1214 (1967)
3. Malofeev V M, Malov O I, Teplykh D A, in *Young Neutron Stars and Their Environments*: *Proc. of the 218th Symp. of the IAU, Sydney, Australia, 14–17 July 2003* (Eds F Camilo, B M Gaensler) (San Francisco, Calif.: Astron. Soc. of the Pacific, 2004) p. 261
4. Malofeev V M et al. *Astron. Zh.* **82** 273 (2005) [*Astron. Rep.* **49** 242 (2005)]

5. Camilo F et al. *Nature* **442** 892 (2006)
6. Goldreich P, Julian W H *Astrophys. J.* **157** 869 (1969)
7. Gurevich A V, Istomin Ya N *Zh. Eksp. Teor. Fiz.* **89** 3 (1985) [*Sov. Phys. JETP* **62** 1 (1985)]
8. Istomin Ya N, Sobyanin D N *Pis'ma Astron. Zh.* **33** 740 (2007) [*Astron. Lett.* **33** 660 (2007)]
9. Beskin V S, Gurevich A V, Istomin Ya N *Physics of the Pulsar Magnetosphere* (Cambridge: Cambridge Univ. Press, 1993)
10. Kramer M et al. *Science* **312** 549 (2006)
11. Gurevich A V, Istomin Ya N *Mon. Not. R. Astron. Soc.* **377** 1663 (2007)

PACS numbers: 63.20.kp, **63.22.–m**
DOI: 10.1070/PU2008v051n08ABEH006597

Multichannel propagation and scattering of phonons and photons in low-dimension nanostructures

Yu A Kosevich

1. Introduction

Recent major achievements in the research and development of technologically and functionally advanced materials have markedly increased research interest in the generation and propagation of coherent acoustic phonons in quasi-one-dimensional superstructures (including those with 'acoustic nanocavities' [1]), nanowires, and nanorods [2]. Of much importance in terms of potential applications is the study of phonon heat transfer in low-dimension systems — for example, through a solid – solid microcontact [3]. The search for technologically feasible materials for thermoelectric transducers lent very topical significance to the recent experimental finding that silicon nanowires with rough surfaces have a much lower thermal conductivity than their smooth-surface counterparts and bulk silicon [4 – 6]. Furthermore, the phonon contribution to the thermal conductivity of single-crystal silicon nanowires with a diameter of less than 50 nm approaches the limiting value found for amorphous silicon, something which current theories cannot explain [5]. Also, the molecular dynamics modeling of the thermal conductivity of diamond nanorods whose surfaces are coated with hydrogen with attached phenyl groups has shown that the thermal conductivity of nanorods is much less than that of bulk crystals [7].

This talk describes and discusses several examples of the so-called multichannel propagation and scattering of phonons and photons, two processes which can contribute to the phonon and photon characteristics, both dynamic and kinetic, of low-dimension systems.

The important thing about the multichannel propagation of phonons or photons is that there are several 'parallel' paths along which propagation is effected, between which both constructive and destructive interference can take place. Path-to-path interference occurring during multichannel propagation in a low-dimension system results in the transmission, reflection, and/or absorption coefficients generally having an asymmetric (non-Lorentzian) line shape as a function of the phonon (photon) frequency.

An asymmetric absorption line shape was first described by Fano [8] in his study of inelastic autoionization resonances in atoms and has been interpreted as due to discrete resonances interfering with the surrounding continuum of 'background' states. Although Fano type asymmetric absorption profiles have been discovered in many atomic systems (see, for example, Ref. [9]), they are not exclusive to them alone and have also been detected in doped semiconductor materials (the absorption [10] and Raman scattering [11] spectra taken from impurities), as well as in bulk intrinsic semiconductor GaAs and semiconductor superlattices [12, 13], and in quantum wells [14]. In the context of electron transport, conductivity as a function of applied voltage or gate voltage has been observed to exhibit asymmetric peaks in quantum dots with few electron levels [15, 16], crossed carbon nanotubes [17], and quantum wires with an attached 'lateral' quantum dot [18, 19]. The electron Fano effect in a quantum dot on one arm of an Aharonov – Bohm interferometer can interact with the Aharonov – Bohm effect [20, 21] and with Kondo correlations in the quantum dot [22]. For photons, the clearest manifestation of the Fano effect is the asymmetrically shaped line of the photon transmission coefficient through a two-dimensional system of local (plasmonic or optical-phonon) resonances [23, 24] or through a layer of a transparent material with a periodic arrangement (two-dimensional lattice) of holes [25, 26].

The phonon analogue of the Fano effect was first described in Ref. [27] and Ref. [28] independently. Reference [27] studied, in particular, the passage of a long acoustic wave (acoustic phonon) through a crystal two-dimensional (2D) defect with a complex structure. A peculiarity in considering such a 2D defect in crystal consisted in accounting for not only the interaction between the neighboring atomic layers closest to the defect but also the direct interaction of the lattice matrix rims through the defect monolayer. In an atomic model of the 2D defect this corresponds to the interaction between nonclosest neighbors. Reference [27] predicted that this essentially monolayer defect characterized by weak local force bondings of both nearest and more distant neighbors can fully reflect in a resonant manner acoustic phonons with wavelengths much larger than the physical thickness of the defect. From the viewpoint of the Fano effect interpretation, the reason for the anomalously strong reflection of an acoustic wave is the destructive interference between two phonon wave paths: through a local oscillator (or through the local bondings of the nearest neighbors) and through the local force bondings of the nonclosest neighbors, bypassing around the local oscillator. A further prediction of Ref. [27] was that a phonon undergoes total resonant absorption (total nonreflection and total nontransmission) at the boundary of a crystal 2D defect with a complex structure. As noted in Ref. [27], a normally incident, long-wave acoustic phonon cannot suffer anomalously strong resonant reflection (or absorption) by a laterally uniform layer of the material (see, for example, the well-known monograph [29]); this can only happen in the acoustics of composite materials. What a laterally uniform layer can only do is resonantly increase the phonon transmission coefficient under Fabry – Perot resonance conditions, thus demonstrating the phonon analogue of the resonant bleaching effect. The interaction of the matrix rims directly through the defect layer is equivalent to the lateral nonuniformity of a two-dimensional defect. Introducing this additional local interaction can also be regarded as effectively taking into account that impurities do not always fill the entire surface of a crystal 2D defect, i.e., impurity atoms can alternate in the plane of the defect with matrix atoms or, alternatively, there may be two or more types of impurities in a 2D defect (Fig. 1).